J. Chem. Sci. Vol. 127, No. 1, January 2015, pp. 61–70.
DOI 10.1007/s12039-014-0750-5

Solvent sorting in (mixed solvent + electrolyte) systems: Time-resolved fluorescence measurements and theory

HARUN AL RASIDGAZI[a], HEMANT K KASHYAP[b] and RANJIT BISWAS[c,*]

[a]Department of Chemistry, Aliah University, Kolkata 700 064, India
[b]Department of Chemistry, Indian Institute of Technology Delhi, Hauz Khas, Delhi 110 016, India
[c]Department of Chemical, Biological and Macromolecular Sciences, S. N. Bose National Centre for Basic Sciences, JD Block, Sector III, Salt Lake, Kolkata 700 098, West Bengal, India
e-mail: ranjit@bose.res.in

MS received 3 July 2014; revised 17 September 2014; accepted 10 December 2014

Abstract. In this manuscript we explore electrolyte-induced modification of preferential solvation of a dipolar solute dissolved in a binary mixture of polar solvents. Composition dependence of solvation characteristics at a fixed electrolyte concentration has been followed. Binary mixtures of two different polarities have been employed to understand the competition between solute-ion and solute-solvent interactions. Time-resolved fluorescence Stokes shift and anisotropy have been measured for coumarin 153 (C153) in moderately polar (ethyl acetate + 1-propanol) and strongly polar (acetonitrile + propylene carbonate) binary mixtures at various mixture compositions, and in the corresponding 1.0 M solutions of $LiClO_4$. Both the mixtures show red shifts in C153 absorption and fluorescence emission upon increase of mole fraction of the less polar solvent component in presence of the electrolyte. In addition, measured average solvation times become slower and rotation times faster for the above change in the mixture composition. A semi-molecular theory based on solution density fluctuations has been developed and found to successfully capture the essential features of the measured Stokes shift dynamics of these complex multi-component mixtures. Dynamic anisotropy results have been analyzed by using both Stokes-Einstein-Debye (SED) and Dote-Kivelson-Schwartz (DKS) theories. The importance of local solvent structure around the dissolved solute has been stressed.

Keywords. Mixed solvent systems; electrolyte solutions; dynamic fluorescence measurements; theory.

1. Introduction

Electrolyte solutions are important reaction media as many biologically relevant reactions occur in these solutions.[1,2] Addition of electrolytes also significantly influences yields of many synthesis and extraction processes in chemical industry.[3–6] In a binary mixture of two polar solvents, polarity can be tuned by changing the composition of the mixture. Again, addition of electrolyte in a given polar solvent or solvent mixture changes average solution polarity. Alteration of mixture composition or addition of electrolyte also modifies the medium viscosity. Viscosity has pronounced effects on solution dynamics. Solvent mixture assists reactivity of a chemical reaction either by increasing the solubility of reactants or through separating the products out of the equilibrium. Although there are several studies[7–19] that investigated the solvation and rotational dynamics either in electrolyte solutions in a single polar solvent or in binary mixtures in the absence of any electrolyte, similar studies for electrolyte solutions in binary polar mixtures are almost non-existent. Such studies are important because understanding the interactions of electrolytes in mixed solvents can provide data that would be useful in many industrial processes for engineering solution properties to tailor a product of a particular reaction. Of course there exist many studies involving electrolytes in binary liquid mixtures that report the bulk thermodynamic properties of solutions.[3–6] Unfortunately these works do not provide any molecular level understanding of the electrolyte interaction-mediated modification in solution structure and dynamics in binary solvent mixtures. Interestingly, electrochemical studies coupled with electrospray ionization (ESI) technique have probed the composition of the first solvation shell around Cu^{+2} ion in aqueous solutions of N,N-dimethylformamide (DMF) and demonstrated that Cu^{+2} ion is preferentially solvated by DMF.[20]

In the case of solvation and rotational dynamics of a dipolar probe in electrolyte solutions of binary solvent mixtures, a competition between two phenomena – preferential solvation[21,22] via probe-solvent interactions and progressive replacement of solvent molecules by

*For correspondence

ions via probe-ion interactions[17] makes the study of solvation processes extremely interesting. This is because varying strength of interactions (ion-dipole versus dipole-dipole) leads to non-linearity in fluorescence emission energy shifts (of a dissolved dipolar probe molecule) in steady state measurements and emergence of a slow component in the time-resolved studies.[21,22] The presence of relatively stronger probe-ion interactions, on the other hand, may soften the non-linearity and can give rise to even slower component in the solvation response due to the slow translational motion of the constituent ions and ion-solvent composite species. If the stronger dipole-ion interaction indeed determines the equilibrium composition of the nearest neighbour around a dipolar solute, the heterogeneity in the solution structure of a binary mixture[23–27] would also be much less sensed by the solvation and rotational dynamics of a dissolved probe. This is because in polar solvation dynamics, the molecular length scale processes contribute at long times when the microscopic solution structure becomes relevant.[28] Thus, a predominance of ion in the nearest neighbour can make the solvation dynamics largely insensitive to the details of the binary solution structure. Consequently, the relevant time resolved decays may not bear the signature of microscopic solution heterogeneity.[23–26,29]

Here we have carried out a composition dependent solvation and rotational dynamics measurements for a dipolar probe, coumarin 153 (C153) in $LiClO_4$ solutions of two binary polar mixtures. These mixtures are composed of ethyl acetate (EA) with propanol (PrOH), and acetonitrile (ACN) with propylene carbonate (PC) at 298 K. The components in each of these binary mixtures are miscible at all mole fractions. While 1.0 M $LiClO_4$ is used to prepare the electrolyte solutions in (EA + PrOH) binary mixtures at all mole fractions, solubility issue restricts us at 0.5 M $LiClO_4$ solutions of (ACN + PC) binary mixtures. These two binary mixtures can be classified as low and strongly polar solutions as the static dielectric constants (ε_0) of EA and PrOH are respectively ~6 and ~20, whereas those for ACN and PC are respectively ~36 and ~65.[30] The difference between these two mixed solvent systems does not lie only in their different polarity values. Data presented in our earlier works[31] have clearly revealed differences in average solution structure between (PrOH + EA) and (PC + ACN) binary mixtures.

The study reported here is motivated by the following questions: (i) can electrolyte modify the environment surrounding the polar probe molecule in a polar binary mixture through the relatively stronger ion-probe interaction? More precisely, how does the stronger ion-probe interaction offset the preferential solvation? (ii) What could be the role of the less polar component in modifying the nearest neighbour arrangements (around the probe molecule) in electrolyte solutions of binary mixtures at varying compositions? This becomes even more pertinent for the mixture containing EA as relatively larger solubility of $LiClO_4$ in EA can significantly modulate the ion-probe interactions and hence affect both the long time dynamics and rotational anisotropy in (EA + PrOH) binary mixtures. (iii) How does this modification in ion-probe interactions vary as one alters the mixture composition? (iv) Does hydrodynamics exclusively control solute rotation in such mixtures?

2. Experimental

ACN, EA, PrOH and PC were used as received (spectrophotometric grade, Aldrich). $LiClO_4$ was obtained (highest available grade, Aldrich) and vacuum dried prior to use. C153 was used as received (Exciton).

Binary mixtures of EA with PrOH, and ACN with PC at several compositions were prepared by dissolving measured amounts of respective components at a given mixture composition. Subsequently, calculated amounts of $LiClO_4$ were dissolved in order to prepare 1.0 M solutions in (EA + PrOH) binary mixtures and 0.5 M solutions in (ACN + PC) binary mixtures at all compositions. The solution viscosities and refractive indices were then measured by using an automated viscometer (Anton Paar, AMVn) and a refractometer (Rudolph, J357) with solution temperature maintained at 293.15 ± 0.5 K.

Details regarding the spectroscopic measurements (steady state and time-resolved) are already described in our earlier works.[31] Typically, sample solutions containing C153 (concentration ~10^{-5} M) were taken in a quartz cell with 1 cm optical path length and absorption spectra were recorded using a UV-VIS spectrophotometer (UV-2450, Shimadzu). Subsequently, emission spectra were recorded (Fluoromax-3, Jobin-Yvon). For solvation dynamics magic angle decays were collected at 18–20 wavelengths[32] via time correlated single photon counting (TCSPC) technique by using 409 nm light as excitation. The full-width at half maximum (FWHM) of the instrument response function (IRF) was ~75 ps. Collected decays were then analyzed following a standard protocol,[32] and the time dependent progress of solvation was expressed in terms of solvation response function, $S(t) = \frac{\nu(t)-\nu(\infty)}{\nu(0)-\nu(\infty)}$, where $\nu(t)$ denotes the frequency (peak or average) of the emission spectrum at a certain time (t) after the laser-excitation of the probe and $\nu(0)$ represents the emission peak frequency immediately after excitation. $\nu(\infty)$ is the peak frequency of

the emission spectrum of the excited probe with fully equilibrated solvent configuration. The average solvation time, $\langle\tau_s\rangle$, was determined from S (t) as follows, $\langle\tau_s\rangle = \int_0^\infty dtS\,(t)$.

Time resolved anisotropy studies were carried out following the standard method. Time resolved fluorescence anisotropies, r(t), were then constructed from the collected parallel ($I_{II}(t)$) and perpendicular ($I_\perp(t)$) decays as follows[33]

$$r(t) = \frac{I_{II}(t) - GI_\perp(t)}{I_{II}(t) + 2GI_\perp(t)}, \tag{1}$$

where G, a geometric factor, was obtained by tail matching the background corrected intensity decays $I_{II}(t)$ and $I_\perp(t)$ and found to be 1.15 ± 0.05. Dynamic anisotropies so obtained were then fitted to bi-exponential functions of time after deconvoluting from the IRF:[33]

$$r(t) = r(0)\left[a_1 \exp(-t/\tau_1) + (1 - a_1)\exp(-t/\tau_2)\right], \tag{2}$$

where τ_i ($i = 1, 2$) represents the time constant associated with each of the decay components (a_i) and r(0) the initial anisotropy which was taken as 0.376.[33] Average rotational correlation time $\langle\tau_{rot}\rangle$ is then obtained via time-integrating r(t)/r(0).

2.1 *Theoretical formulation and calculation details*

Here we begin by writing the expression for the total excess free energy functional for systems where we model solute and solvent molecules as dipolar hard spheres and dissociated ions as charged hard spheres.[27,34–39] We approximate the mixture of the dipolar solvents as an effective single component dipolar liquid that is characterized by an effective dipole moment $\mu_{eff} = (x_1\mu_1^2 + x_2\mu_2^2)^{1/2}$ and size $\sigma_{eff} = (x_1\sigma_1^3 + x_2\sigma_2^3)^{1/3}$. Here x_i, μ_i and σ_i are the mole fraction, dipole moment and diameter of i^{th} type solvent molecules, respectively. In addition, complete dissociation of the dissolved electrolyte is assumed.

The expression for the position (**r**), orientation (Ω) and time (t) dependent solvation energy of mobile dipolar solute with density distribution $\rho_s(\mathbf{r}, \Omega; t)$ is given by[35–39]

$$\begin{aligned}\Delta E_{total}(\mathbf{r}, \Omega; t) &= -k_B T \rho_s(\mathbf{r}, \Omega; t) \\ &\times \left[\int d\mathbf{r}' d\Omega' c_{sd}(\mathbf{r}, \Omega; \mathbf{r}', \Omega')\delta\rho_d(\mathbf{r}', \Omega'; t)\right. \\ &\left. + \sum_{\alpha=1}^{2}\int d\mathbf{r}' c_{s\alpha}(\mathbf{r}, \Omega; \mathbf{r}')\delta n_\alpha(\mathbf{r}'; t)\right] \\ &= \Delta E_{sd}(\mathbf{r}, \Omega; t) + \Delta E_{si}(\mathbf{r}, \Omega; t)\end{aligned} \tag{3}$$

where $c_{sd}(\mathbf{r}, \Omega; \mathbf{r}', \Omega')$ and $c_{s\alpha}(\mathbf{r}, \Omega; \mathbf{r}')$ are respectively the position and orientation dependent solute dipole-solvent dipole (dipole-dipole) and solute dipole-ion (dipole-ion) direct correlation functions[40,41] and α denotes the type of ions (cation and anion). The fluctuations in dipolar density ($\delta\rho_d$) and ion density (δn_α) from the respective bulk values are defined as follows: $\delta\rho_d(\mathbf{r}, \Omega) = \rho_d(\mathbf{r}, \Omega) - \rho_d^0/4\pi$ and $\delta n_\alpha(\mathbf{r}) = n_\alpha(\mathbf{r}) - n_\alpha^0$. Therefore, the solvation energy-energy correlation function averaged over space (**r**) and orientation (Ω) for such system is written as

$$C_E(t) = C_{sd}(t) + C_{si}(t), \tag{4}$$

where $C_{sd}(t)$ and $C_{si}(t)$ are the energy-energy correlation functions for dipole-dipole and dipole-ion interactions, respectively. Analytical expressions for $C_{sd}(t)$, $C_{si}(t)$ and other details are provided in the Supporting Information. Subsequently, the expression for the normalized total solvation response function is written as

$$\begin{aligned}S_E(t) = &\frac{C_{sd}(t=0)}{[C_{sd}(t=0) + C_{si}(t=0)]}S_{sd}(t) \\ &+ \frac{C_{si}(t=0)}{[C_{sd}(t=0) + C_{si}(t=0)]}S_{si}(t)\end{aligned} \tag{5}$$

where $S_{sd}(t) = \frac{C_{sd}(t)}{C_{sd}(t=0)}$ and $S_{si}(t) = \frac{C_{si}(t)}{C_{si}(t=0)}$ are the normalized solvation energy auto-correlation functions due to dipole-dipole and dipole-ion interactions between the solute and dipolar solvent species, and between the solute and ions, respectively. Other parameters necessary for calculations are provided in Appendix 1 of the Supporting Information.

3. Results and Discussion

3.1 *Steady state studies*

Representative absorption and emission spectra of C153 in EA, PrOH and 50:50 mixture of (EA + PrOH) in the presence and absence of electrolyte ($LiClO_4$) are shown in figure 1. (Similar spectra for binary mixtures of ACN in PC are provided in figure S1 of the Supporting Information). As expected, the shift in the absorption spectrum is much less than that in emission as either the solvent composition is changed or electrolyte added. Note in figure 1 that relative to pure solvents, addition of 1.0 M $LiClO_4$ red-shifts the emission spectrum in ethyl acetate by $\sim$1500 cm^{-1} whereas the same addition of electrolyte in PrOH shifts the spectrum by only $\sim$300 cm^{-1}, even-though the dielectric constant of PrOH is almost three times larger than that of EA. This probably suggests more direct probe-electrolyte

interactions in EA due to relatively less dielectric screening by solvents of lower polarity. In fact, the separation between the emission peak frequencies in the absence and presence of $LiClO_4$, increases as the mole fraction of EA is increased in (EA + PrOH) binary mixtures.

The above feature is more clearly shown in figure 2 where the absorption and emission peak frequencies and the spectral widths in the presence and absence of $LiClO_4$ are presented as a function of mole fraction of the less polar solvent (EA or ACN). Note that in figure 2, (i) addition of electrolyte in both these mixtures induces extra stabilization (red-shift) of absorption and emission spectra of the dissolved probe, the extent of stabilization being more in the electrolyte solutions of the relatively less polar solvent components, (ii) in presence of 1.0 M $LiClO_4$, the emission peak frequency of C153 in (EA + PrOH) binary mixtures remains almost constant at all EA mole fractions, (iii) the widths of the absorption spectra in these mixtures in the presence and absence of electrolyte are larger than emission bandwidths which has already been observed in neat solvents[32] and electrolyte solutions of single polar solvents,[17] (iv) even though the variation in width is very small (within a few hundred cm^{-1}), emission spectrum in presence of electrolyte at all mole fractions appears to be narrower than in the absence of electrolyte, and (v) the effects of electrolyte on both spectral shift and width are weaker in (ACN + PC) mixture than in the other binary mixture.[42]

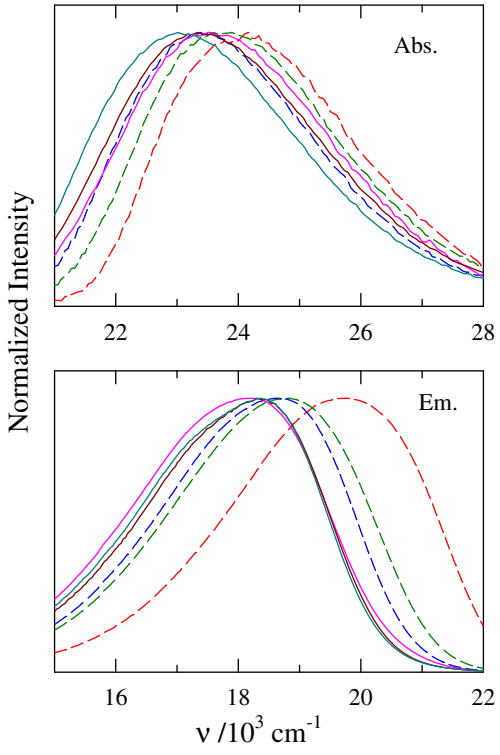

Figure 1. Representative absorption (upper panel, 'Abs.') and emission spectra (lower panel, 'Em.') of C153 in (ethyl acetate + propanol) binary mixtures in presence (solid line) and absence (dashed line) of 1.0 M $LiClO_4$. Red, green and blue lines represent spectra in pure ethyl acetate, 50:50 mixture of (ethyl acetate + propanol) and pure propanol, respectively. Pink, dark red, dark cyan lines represent spectra in pure ethyl acetate, 50:50 mixture of (ethyl acetate + propanol) and pure propanol in presence of 1.0 M $LiClO_4$, respectively.

3.2 *Time resolved studies: Solute solvation*

Experimental studies have indicated that the polar solvation dynamics of the pure solvents considered here are characterized by multi-exponential decays consisting of fast components with time constants in the range of sub-hundred femtosecond to sub-picosecond.[32] In addition, the experimental average solvation times ($\langle\tau_s\rangle$) for EA and ACN are found to be in the sub-picosecond regime whereas those for PC and PrOH are 2 ps and 26 ps, respectively.[32] Therefore, the binary mixtures of these fast solvents and also the electrolyte solutions of them (binary mixtures) are expected to have large fast components which are likely to be

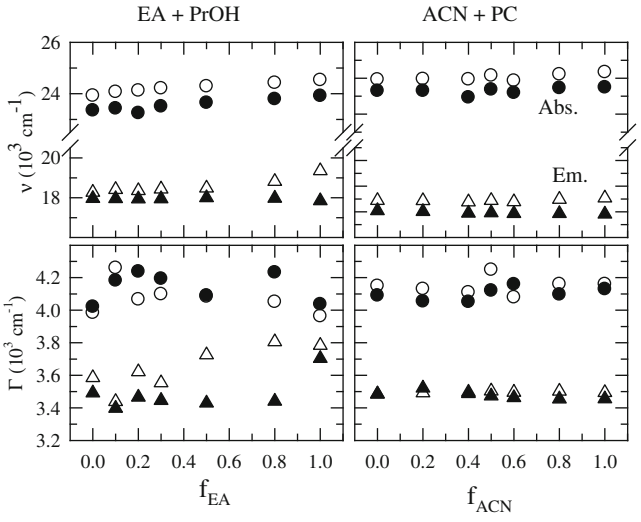

Figure 2. Spectral characteristics of C153 in binary mixtures of (ethyl acetate + propanol), (left panel) and (acetonitrile + propylene carbonate) (right panel). Upper panels present mole fraction dependence of absorption and emission peak frequencies and lower panels depict the full width at half maxima (fwhm) of the absorption and emission spectra. Open circles and filled circles denote absorption in the absence and presence of $LiClO_4$. Open triangles and filled triangles represent emission in absence and presence of $LiClO_4$. Note that the concentrations of $LiClO_4$ in (ethyl acetate + propanol) and (acetonitrile + propylene carbonate) mixtures respectively are 1.0 M and 0.5 M.

missed by the broad time resolution employed in the present experiments. This is the reason for the solvation response functions obtained in our experiments being single exponential for all these mixtures and electrolyte solutions studied here. The composition dependent $\langle\tau_s\rangle$ for (EA + PrOH) binary mixtures determined from our experiments in the presence and absence of $LiClO_4$ are summarized in table 1 where estimated missing fractions[43] of the total solvation response function in these systems are also indicated. Representative time resolved emission spectra[32] at a particular mixture composition are shown in figure S2 of the Supporting Information. As expected, in the absence of the electrolyte $\langle\tau_s\rangle$ for (EA + PrOH) decreases (table 1a) very slowly with the increase in EA mole fraction, and almost all of the solvation response is missed when the system becomes pure EA. Note also that $\langle\tau_s\rangle$ measured in our experiments for propanol is almost twice than that reported in earlier studies.[32] This is because the present experiments can detect only the slow part (∼50%) of the total solvation response in propanol that decays with a time constant of approximately 50 ps.[32]

However, the solvation dynamics in presence of electrolyte becomes slower as translational motions of both ion and ion-solvent composites contribute. Data in table 1b indicate that $\langle\tau_s\rangle$ in presence of 1.0 M $LiClO_4$ remains almost insensitive to the solvent composition till the EA mole fraction become 0.5 in the mixture and then increases sharply. The near insensitivity of $\langle\tau_s\rangle$ to EA mole fraction in the presence and absence of $LiClO_4$ is probably due to the missing of a significant portion of the initial fast response in each of these systems. However, $\langle\tau_s\rangle$ obtained here for 1.0 M $LiClO_4$ solution in EA and that for ACN in presence of 0.5 M $LiClO_4$ (∼600 ps, not shown here) are comparable with those[17] in ACN and THF (tetrahydrofuran) in presence of 1.0 M $NaClO_4$. Note also that in table 1, in presence of $LiClO_4$ at each EA mole fraction the magnitude of missing component is larger than that in the absence of it even though the $\langle\tau_s\rangle$ are larger in the former systems than the latter. The following could be the reasons for this behaviour: (i) although the long time dynamics becomes slower due to the participation of translational motions of the ions, the presence of substantial fraction of ion-pairs[7–10] in 1.0 M $LiClO_4$ solutions increases the weight of the polar solvation energy relaxation via the relatively faster rotational motion of these ion-pairs. As a result, a larger fraction of this fast dynamics is missed; (ii) as $LiClO_4$ is insoluble in the non-polar reference (hexane) used in the present study, the effects of increased density upon addition of electrolyte is missing in the non-polar reference spectra.[31a] Consequently,

Table 1. Mole fraction dependent average solvation times, dynamic Stokes shift for C153 (both observed and 'true') and percentage of missing components of total solvation response function in binary mixtures in the presence and absence of 1.0 M $LiClO_4$.

A. (Ethyl acetate + Propanol) mixtures				
Mole fraction of ethyl acetate	$\langle\tau_s\rangle$ (ps)	Observed $\Delta\nu$(t) (cm^{-1})	True $\Delta\nu$(t) (cm^{-1})	% missed (approx.)
0.0	57	1309	1876	30
0.1	52	1179	1892	38
0.2	44	1254	1963	36
0.3	50	984	1995	51
0.5	50	972	1977	51
0.8	47	748	1759	57
1.0	33	50	1332	96
B. (Ethylacetate + Propanol +1.0 M $LiClO_4$) mixtures				
Mole fraction of ethyl acetate	$\langle\tau_s\rangle$ (ps)	Observed $\Delta\nu$(t) (cm^{-1})	True $\Delta\nu$(t) (cm^{-1})	% missed (approx.)
0.0	126	1272	2020	37
0.1	117	1003	1907	47
0.2	121	759	1738	56
0.3	123	944	2002	53
0.5	154	986	2172	55
0.8	307	863	2478	65
1.0	692	849	2886	71

the estimate of the time-zero spectrum becomes much less quantitative.

Calculated solvation response functions, $S_E(t)$ from Eq. 5, for (EA+PrOH) mixture and its 1 M $LiClO_4$ solution at various mole fractions of EA are shown in the *upper* and *lower* panels of figure 3, respectively. The predicted S_E (t) for (ACN+PC) mixtures with and without 0.5 M $LiClO_4$ is shown in figure S3. The individual components due to dipole-dipole interaction, $S_{sd}(t)$, and dipole-ion interaction, $S_{si}(t)$, for $LiClO_4$ solutions of these binary solvent mixtures are provided in figures S4 and S5, respectively. Data in these figures clearly show that with increasing less polar solvent component in the solvent mixture the solvation response becomes faster. Note the predicted response functions are non-exponential although the experimental ones are single exponential functions of time. The reason for this difference is the incomplete detection of the full solvation response due to the limited instrumental resolution employed. Calculated $S_E(t)$ are tri-exponential for (EA + PrOH) and bi-exponential for (ACN+PC) mixtures. Calculated response functions for the corresponding $LiClO_4$ solutions of the two mixed solvent systems

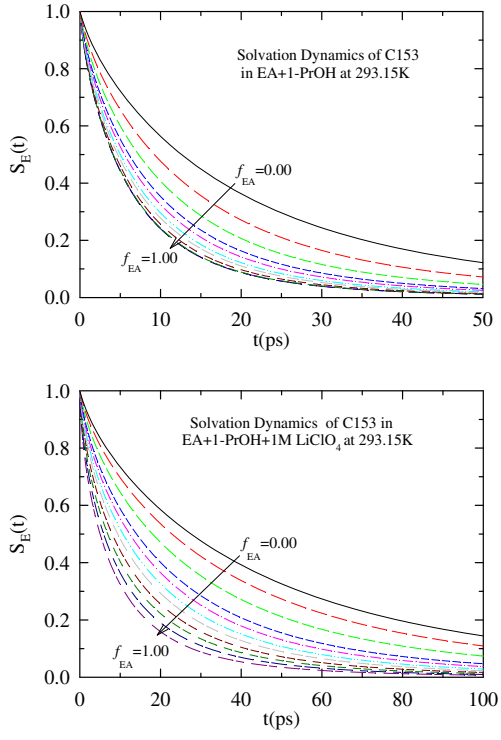

Figure 3. Theoretically constructed total solvation response function, $S_E(t)$, at eleven different EA mole fractions in the absence (upper panel) and presence (lower panel) of the electrolyte in (EA+PrOH) binary mixtures. The arrow indicates the increase in EA mole fraction by 0.1 intervals. Representations are colour coded.

follow the same trends. $\langle\tau_s\rangle$ predicted for pure PrOH is ~22 ps which agrees well with a value of 26 ps, obtained via complete measurements.[32] The details of the time constant associated with the individual solvent response of the two solvent mixtures both in presence and absence of electrolyte are shown in the tables S4 and S5.

Let us now explore the origin of solvation time scales predicted by the model calculations. Three distinct time scales of $S_E(t)$ in (EA+PrOH) binary mixtures for both in presence and absence of electrolyte are obtained. The larger two timescales (τ_2 and τ_3) originate from the diffusive rearrangement of the environment surrounding the solute in these binary mixtures. The fastest one (τ_1) arise from the collective rotation of dipolar solvent molecules. Increase of the longer timescales upon addition of electrolyte arises from the increase in solution viscosity. Two separate solvation time scales in (ACN + PC) binary mixtures both in presence and absence of electrolyte may arise from a combination of solvent rotation and translation, and translation of ions. Calculated $\langle\tau_s\rangle$ for these two mixed solvent systems in presence and absence of electrolyte are shown in figure 4. This figure clearly shows that the presence of electrolyte slows down $\langle\tau_s\rangle$ in both the mixtures. Interestingly, such a slowing down of solvation timescales has not been observed in the present experiments. This may indicate over-estimation of ion-dipole interaction contribution to the solvation energy relaxation in electrolyte solutions of these binary solvent systems. In addition, the separation of dipolar part of the solvation energy fluctuation from the ion-dipole contribution[44] (as envisaged here) may not be completely valid and is arbitrary to some extent. However, the fact that the solvent rotation being much faster than the ion translation provides some support to this approximation.[19,45,46]

Experimentally determined electrolyte effects on dynamic Stokes shift in (EA + PrOH) binary mixtures are shown in figure 5. While data in the *upper panel* indicate the electrolyte contribution, those in the *middle panel* represent the total dynamic Stokes' shift in presence of 1.0 M $LiClO_4$. Interestingly, this figure represents the increase in dynamic stokes shift with increase in less polar solvent component of the mixture although the reverse is expected. This anomalous result can be explained in terms of the inverse Debye screening length, κ_D, shown in *lower panel*. Inverse Debye screening length increases with increase of less polar solvent component which means that Debye screening length decreases with increase in less polar solvent component. This in turn facilitates interaction between the solute dipole and the dissociated ions around, increasing the Stokes shift magnitude.

3.3 *Time resolved studies: Solute rotation*

We next present the results on composition dependent average rotational correlation times in these mixtures in the presence and absence of the electrolyte. The decay of the time resolved fluorescence anisotropy (r(t)) at each composition in these binary mixtures has been found to be bi-exponential function of time, irrespective of the presence or absence of the electrolyte. Earlier studies of fluorescence anisotropy with C153 in pure polar solvents[33] and aqueous tertiary butanol mixtures[26] have also reported bi-exponential decay of r(t). The average rotational correlation times ($\langle\tau_{rot}\rangle$) obtained from the present study for the solute C153 in (EA + PrOH) and (ACN + PC) binary mixtures are shown as a function of mole fraction of the relatively less polar components in the *upper panel* of figure 6. The *lower panel* of figure 6 shows the variation of $\langle\tau_{rot}\rangle$ as a function of composition dependent solution viscosity (figure S6 and tables S1/S2). Note that $\langle\tau_{rot}\rangle$ values (triangles) for (ACN + PC) mixtures in the absence of $LiClO_4$ are taken from literature.[18] In both these mixtures in presence and absence of the electrolyte, $\langle\tau_{rot}\rangle$ decreases exponentially with the mole fraction of either EA or ACN in these mixtures. The exponential mole fraction dependence of $\langle\tau_{rot}\rangle$ has already been reported for a few binary mixtures studied with both charged[16] and neutral solute probes.[18] We would like to mention here that the values of $\langle\tau_{rot}\rangle$ of C153 in pure EA and PrOH are agreeing well with the literature values.[33]

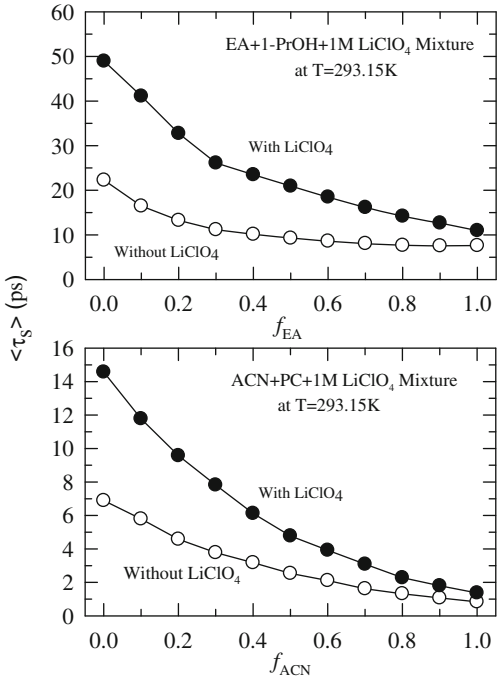

Figure 4. Mole fraction (of the relatively less polar component in the binary mixtures) dependence of theoretical average solvation time, $\langle\tau_s\rangle$ of C153 in (EA + PrOH) binary mixtures (upper panel, 'EA+PrOH') and (ACN + PC) binary mixture (lower panel, 'ACN+PC'). Open and filled circles represent $\langle\tau_s\rangle$ in the absence and presence of 1.0 M $LiClO_4$, respectively in (EA + PrOH) binary mixtures. Open and filled triangles represent $\langle\tau_s\rangle$ for the other binary mixture in the absence and presence of 1.0 M $LiClO_4$, respectively.

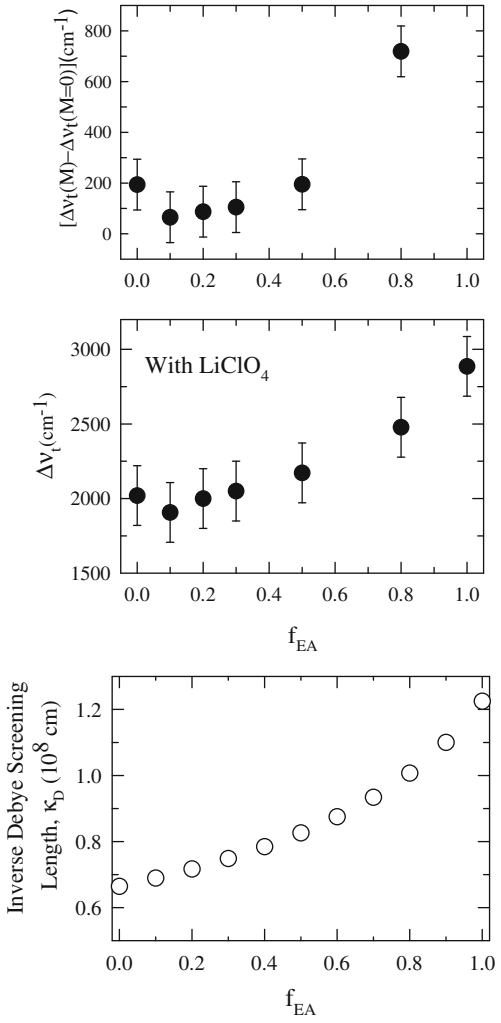

Figure 5. Mole fraction (of the relatively less polar component in the binary mixtures) dependence of dynamic Stokes shift of C153 in (EA + PrOH) binary mixtures only due to the electrolyte (*upper panel*) and total dynamic Stokes' shift in the 1.0 M $LiClO_4$ solution of the same mixture (*middle panel*). Note that the dynamic Stokes shift is calculated from the peak frequencies of the synthesized emission spectrum at t = 0 (ν (0)) and emission spectra at t = ∞($\nu(\infty)$) spectra of C153 as follows: $\Delta\nu_t = \nu(0) - \nu(\infty)$. Stokes shift caused by the electrolyte only is equal to $\Delta\nu_t(M) - \Delta\nu_t(M = 0)$, where $\Delta\nu_t(M)$ and $\Delta\nu_t(M = 0)$ denote the dynamic Stokes shift in the presence and absence of the electrolyte, respectively. The *lower panel* of the figure represents the less polar solvent (EA) component dependence of calculated inverse Debye screening length.

The exponential increase of $\langle\tau_{rot}\rangle$ with solution viscosity (lower panel, figure 6) indicates either the change in hydrodynamic boundary condition[16] or contribution of the rotational dielectric friction[12–15] to the total resistance experienced by the rotating solute in solution. Although the dielectric friction aspect has already been investigated for charged solute in electrolyte solutions of a single component solvent[12–15] and for neutral solute in supercritical solvents,[47] such studies with neutral dipolar solute in electrolyte solutions of binary polar mixtures have not been investigated yet. The well known Stokes-Einstein-Debye (SED) theory provides the following expression for rotational time,[33]

$$\tau_r = \frac{\eta v f C}{k_B T}, \tag{6}$$

where η is the medium viscosity, v the solute volume, k_B the Boltzmann constant and T the absolute temperature. f and C are the shape factor and solute-solvent coupling parameter, respectively. The average rotational correlation times ($\langle\tau_{rot}\rangle$) obtained from the experiments, SED-predicted rotation times at two different boundary conditions and SED-predicted rotation times in the stick limit for a spherical solute with volume of C153 in (EA + PrOH) and (ACN + PC) binary mixtures both in presence (*lower panel*) and absence (*upper panel*) of electrolyte are shown in figure 7 as a function of mole fraction of the relatively less polar components in these two binary mixtures. Experimental rotational time lies in between stick and slip hydrodynamic limits for all the systems. Interestingly, the figure shows that SED predicted rotational time matches well with the experimental values of rotational time obtained in experiments when the solute is taken as spherical ($f = 1$) and coupling parameter C is considered in the stick boundary limit (C = 1).

The above observation raises the following question: why does the SED provide such a good description of experimental rotation times in the limit of spherical solute diffusion under the stick boundary condition? C153 possesses the shape of an ellipsoid with semi-axes dimensions of 2.0, 4.8 and 6.1 Å.[33] So, the shape factor, should be greater than unity and the coupling parameter less than unity (that is, f > 1 and C < 1). Hence, the agreement between SED predictions and experimental data might originate from the partial cancellation of the shape factor and the solute-solvent coupling parameter. The performance of the Dote-Kivelson-Schwartz

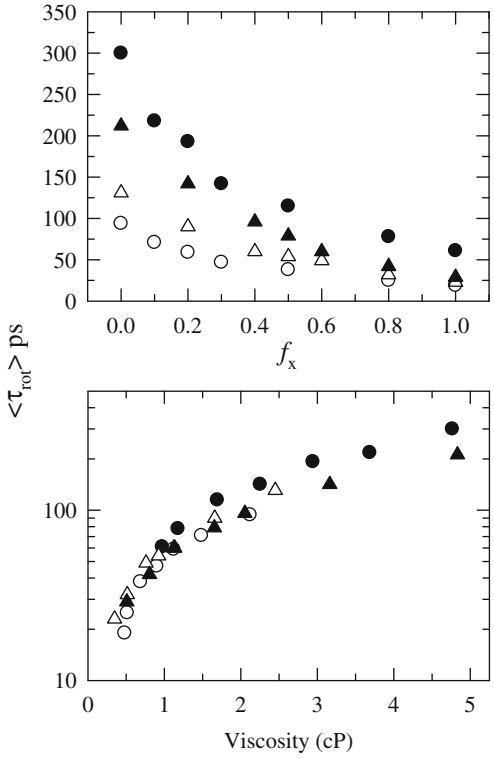

Figure 6. Mole fraction (of the relatively less polar component in the binary mixtures) dependence of rotational time C153 in two binary mixtures (EA+PrOH and ACN+PC) in upper panel whereas lower panel represents the solution viscosity dependence of the same. Open and filled circles represent average rotational times of C153 in (EA + PrOH) binary mixtures in the absence and presence of 1.0 M $LiClO_4$, respectively. Open and filled triangles represent the same in (ACN + PC) binary mixtures in the absence and presence of 0.5 M $LiClO_4$, respectively.

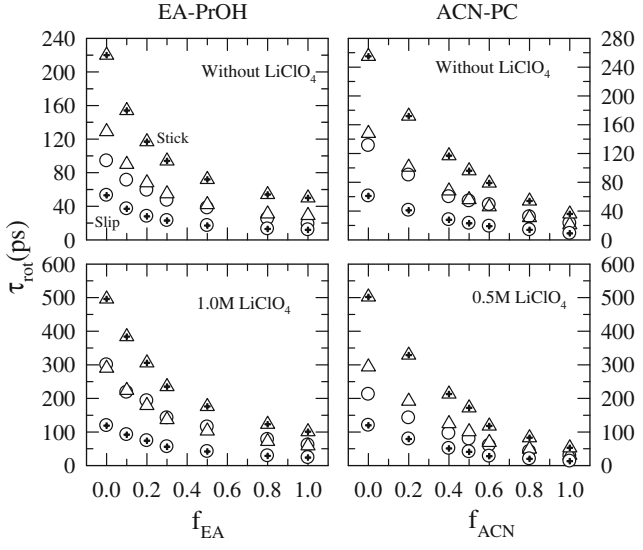

Figure 7. Predictions from stick (triangle crossed) and slip (circle crossed) hydrodynamics for solute rotation times with proper shape factor of C153 ($f = 1.71$) in these binary mixtures in the presence and absence of electrolyte, and comparison with experimental data (circles). Triangles in each panel represent predicted rotational times using stick boundary condition assuming spherical solute.

(DKS)[48] theory for predicting C153 rotation times in these systems are presented in figure S7 and discussed in Appendix 2 of the Supporting Information.

Local structure around a solute (first solvation shell) can be different from that in the bulk solution. The inhomogeneity in mixed solvent system is well known.[49] Signatures of local environment surrounding a dissolved solute are reflected in static absorption and emission spectral characteristics. Now if the effects of local environment are incorporated somehow in the calculations of C, then a better agreement between theory and experiments is expected. For example, if the C values from DKS are increased by adding ~20% of the relative Stokes shift (that is, $C_{mod} = C_{DKS} + \Delta C$, $\Delta C = 0.2x(\Delta\Delta\nu/cm^{-1})$) at any composition of these two different mixed solvent systems in the absence and presence of the electrolyte, a much better agreement results. Even though this way for modification of C is purely ad-hoc, the observation indicates the importance of local solvent structure for solute rotation in solutions. This, in turn, suggests inclusion of modified solvent structure[50] and subsequent effects on angular diffusion in presence of long-ranged interactions. Such a work assumes even more importance given that a quasi-universality in solute rotation for a wide variety of solute-medium combinations has been reported in a recent theoretical study.[29]

4. Conclusion

In this article, solvation and rotational dynamics of C153 have been investigated in two different kinds of mixed solvent systems: mixtures of EA and PrOH, and mixtures of ACN and PC. These two are different on average polarity ground. Steady state spectroscopic studies in these mixtures have revealed stronger electrolyte effects in the lower polarity binary mixture than in the higher polarity counterpart. Also, addition of electrolyte increases the Stokes shift linearly in the lower polarity binary mixture with the increase of mole fraction of the relatively less polar solvent component. Such behaviour is not observed in electrolyte solutions of the higher polarity binary mixture.

Solvation dynamics studies in these binary mixtures in the presence and absence of the electrolyte have indicated a significant fraction of the dynamics being missed at each solvent composition due to the limited time resolution employed. Our semi-molecular theory is in qualitative agreement with experimental results, providing qualitative explanations of solvation timescales observed in experiments. The average rotational correlation time has been found to show exponential mole fraction (of the less polar component) dependence in the presence and absence of the dissolved electrolyte for both of these binary mixtures. However, the rotational correlation times in these binary mixtures deviate from linearity when plotted as a function of solution viscosity, indicating modifications in solute-solvent coupling. While development of a full molecular theory for studying rotational dynamics in such complex solutions is a challenging task, computer simulation studies with proper modeling of the interactions are expected to generate a better understanding of these and similar systems.[51–56] The heterogeneity aspects of these solutions and their subsequent effects on dynamics[57–61] need to be studied as measurements of perchlorate solutions of these solvents indicate fascinating information on solvent-electrolyte interactions.[62–66]

Supplementary information

The electronic supporting information can be seen at www.ias.ac.in/chemsci.

Acknowledgement

HG thanks the Vice-Chancellor, Aliah University, Kolkata for encouragement. HKK would like to thank IRD unit, IIT-Delhi for financial support.

References

1. Robinson R A and Stokes R H 1959 In *Electrolyte Solutions* 2nd edition. (London: Butterworth)
2. Birch N J 1999 *Chem. Rev.* **99** 2659
3. Marcus Y and Hefter G 2006 *Chem. Rev.* **106** 4585
4. Marcus Y and Hefter G 2004 *Chem. Rev.* **104** 3405
5. Hefter G, Marcus Y and Waghorne W E 2002 *Chem. Rev.* **102** 2773
6. Kalidas C, Hefter G and Marcus Y 2000 *Chem. Rev.* **100** 819
7. Bart E and Huppert D 1992 *Chem. Phys. Lett.* **195** 37
8. Huppert D, Ittah V and Kosower E M 1989 *Chem. Phys. Lett.* **159** 267
9. Ittah V and Huppert D 1990 *Chem. Phys. Lett.* **173** 496
10. Pradhan T and Biswas R 2007 *J. Phys. Chem. A* **111** 11524
11. Hartman R S, Konitsky W M and Waldeck D H 1993 *J. Am. Chem. Soc.* **115** 9692
12. Balabai N, Kurnikova M G, Coalson R D and Waldeck D H 1998 *J. Am. Chem. Soc.* **120** 7944
13. (a) Balabai N and Waldeck D H 1997 *J. Phys. Chem.* **101** 2339; (b) Hartman R S and Waldeck D H 1994 *J. Phys. Chem.* **98** 1386

14. (a) Pardhan T, Gazi H A R and Biswas R 2009 *J. Chem. Phys.* **131** 054507; (b) Pardhan T, Gazi H A R, Gucchait B and Biswas R 2012 *J. Chem. Sci.* **124** 355
15. (a) Hartman R S, Alavi D S and Waldeck D H 1991 *J. Phys. Chem.* **95** 7872; (b) Alavi D S and Waldeck D H 1991 *J. Phys. Chem.* **95** 4848
16. (a) Guchhait B and Biswas R 2013 *J. Chem. Phys.* **138** 114909; (b) Pradhan T and Biswas R 2009 *J. Solution Chem.* **38** 517
17. Chapman C F and Maroncelli M 1991 *J. Phys. Chem.* **95** 9095
18. Gardecki J A and Maroncelli M 1999 *Chem. Phys. Lett.* **301** 571
19. Chandra A 1995 *Chem. Phys. Lett.* **244** 314
20. Tsierkezos N G, Roithova J, Schröder D, Molinou I E and Schwarz H 2008 *J. Phys. Chem. B* **112** 4365
21. Molotsky T and Huppert D 2002 *J. Phys. Chem.* **106** 8525
22. Khajehpour M and Kauffman J F 2000 *J. Phys. Chem. A* **104** 7151
23. Beddard G S, Doust T and Hudales J 1981 *Nature* **294** 145
24. Soper A K and Finney J L 1993 *Phys. Rev. Lett.* **71** 4346
25. Pradhan T, Ghoshal P and Biswas R 2008 *J. Phys. Chem. A* **112** 915
26. Pradhan T, Ghoshal P and Biswas R 2008 *J. Chem. Sci.* **120** 275
27. Daschakraborty S and Biswas R 2014 *J. Chem. Phys.* **140** 014504
28. Bagchi B and Biswas R 1999 *Adv. Chem. Phys.* **109** 207
29. (a) Das A, Biswas R and Chakrabarti J 2012 *J. Chem. Phys.* **136** 014505; (b) Das A, Biswas R and Chakrabarti J 2013 *Chem. Phys. Lett.* **558** 36
30. Gazi H A R and Biswas R 2011 *J. Chem. Sci.* **123** 265
31. (a) Guchhait B, Biswas R, and Ghorai P K 2013 *J. Phys. Chem. B* **117** 3345; (b) Biswas R, Das A R, Pradhan T, Touraud D, Kunz W and Mahiuddin S 2008 *J. Phys. Chem. B* **112** 6620; (c) Guchhait B, Das S, Daschakraborty S and Biswas R 2014 *J. Chem. Phys.* **140** 104514; (d) Guchhait B, Daschakraborty S and Biswas R 2012 *J. Chem. Phys.* **136** 174503
32. Horng M L, Gardecki J A, Papazyan A and Maroncelli M 1995 *J. Phys. Chem.* **99** 17311
33. Horng M L, Gardecki J A and Maroncelli M 1997 *J. Phys. Chem. A* **101** 1030
34. Chandra A and Bagchi B 1999 *J. Chem. Phys.* **110** 10024
35. (a) Kashyap H K and Biswas R 2008 *J. Phys. Chem. B* **112** 12431; (b) Kashyap H K and Biswas R 2010 *J. Phys. Chem. B* **114** 254
36. Kashyap H K and Biswas R 2010 *J. Phys. Chem. B* **114** 16811
37. Kashyap H K and Biswas R 2010 *Ind. J. Chem.* **49A** 685
38. (a) Daschakraborty S and Biswas R 2014 *J. Phys. Chem. B* **118** 1327; (b) Daschakraborty S and Biswas R 2011 *J. Phys. Chem. B* **115** 4011
39. Guchhait B, Gazi H A R, Kashyap H K and Biswas R 2010 *J. Phys. Chem. B* **114** 5066
40. Gray C G and Gubbins K E 1984 In *Theory of Molecular Fluids* Vol. I (Oxford: Clarendon)
41. Hansen J P and McDonald I R 1986 In *Theory of Simple Liquids* (London: Academic)
42. Pradhan T and Biswas R 2007 *J. Phys. Chem. A* **111** 11514
43. Fee R S and Maroncelli M 1994 *Chem. Phys.* **183** 235
44. Chapman C F and Maroncelli M 1991 *J. Phys. Chem.* **95** 9095
45. Chapman C F, Fee R S and Maroncelli M 1995 *J. Phys. Chem.* **99** 4811
46. Chandra A and Patey G N 1994 *J. Chem. Phys.* **100** 1552
47. Das A, Biswas R and Chakrabarti J 2011 *J. Phys. Chem. A* **115** 973
48. Dote J L, Kivelson D and Schwartz R N 1981 *J. Phys. Chem.* **85** 2169
49. Berg M and Vanden Bout D A 1997 *Acc. Chem. Res.* **30** 65
50. Daschakraborty S and Biswas R 2012 *J. Chem. Sci.* **124** 763
51. Nag A, Kundu T, Bhattacharyya K 1989 *Chem. Phys. Lett.* **160** 257
52. Banerjee S, Roy S and Bagchi B 2010 *J. Phys. Chem. B* **114** 12875
53. Roy S, Banerjee S, Biyani N, Jana B and Bagchi B 2011 *J. Phys. Chem. B* **115** 685
54. Roy S, Jana B and Bagchi B 2012 *J. Chem. Phys.* **136** 115103
55. Ghosh R, Banerjee S, Chakrabarty S and Bagchi B 2011 *J. Phys. Chem. B* **115** 7612
56. Roy S and Bagchi B 2013 *J. Chem. Phys.* **139** 034308
57. Das A, Das S and Biswas R 2013 *Chem. Phys. Lett.* **581** 47
58. Guchhait B, Das S, Daschakraborty S and Biswas R 2014 *J. Chem. Phys.* **140** 104514
59. Pal T and Biswas R 2011 *Chem. Phys. Lett.* **517** 180
60. Pal T and Biswas R 2013 *Theor. Chem. Acc.* **132** 1348
61. Pal T and Biswas R 2014 *J. Chem. Phys.* **141** 104501
62. Eberspächer P, Wismeth E, Buchner R and Barthel J 2006 *J. Mol. Liq.* **129** 3
63. Barthel J, Neueder R, Poxleitner M, Seitz-Beywl J and Werblan L 1993 *J. Electroanal. Chem.* **344** 249
64. Barthel J, Iberl L, Rossmaier J, Gores H.-J and Kaukal B 1990 *J. Solution Chem.* **19** 321
65. Wachter R and Riederer K 1981 *Pure Appl. Chem.* **53** 1301
66. Salomon M, Slane S, Plichta E and Uchiyama M 1989 *J. Solution Chem.* **18** 977